Biointerface Research in Applied Chemistry
Open-Access Journal (ISSN: 2069-5837)

Article
Volume 14, Issue 5, 2024, 116
https://doi.org/10.33263/BRIAC145.116

Characterization and Applications of Silver Nanoparticles Photosynthesized from *Durio* Zibethinus Peel Extract

Trung Dien Nguyen [1,*], Nhut Minh Pham [1], Nhung Thi-Tuyet Thai [1], Huong Thi-Thu Nguyen [1], Yen Hai Hoang [1], Anh Cam Ha [2]

[1] School of Education, Can Tho University, 3/2 Street, Ninh Kieu, Can Tho City, 94000, Vietnam
[2] Ho Chi Minh City University of Technology, Vietnam National University Ho Chi Minh City, 268 Ly Thuong Kiet Street, Ho Chi Minh City, 72500, Vietnam
* Correspondence: ndtrung@ctu.edu.vn;

Scopus Author ID 57224777781
Received: 7.11.2023; Accepted: 28.01.2024; Published: 21.07.2024

Abstract: The present study investigated the photochemical synthesis of silver nanoparticles using the extract from *Durio zibethinus* peels with blue light-emitting diode irradiation. *Durio zibethinus* peel extract is a reducing and stabilizing agent that forms silver nanoparticles. Silver nanoparticle formation was detected at a maximum wavelength of 423 nm in the UV-visible spectrum. Under the optimized synthesis conditions, silver ions were reduced to silver nanospheres with an average diameter of 13.3 nm. The produced silver nanoparticles are highly stable in 10 weeks for storage with a zeta potential of –20.4 mV and stabilized by phenolics in the presence of extract through Fourier transform infrared analysis. Nanomaterials synthesized from *Durio zibethinus* peel extract have a high inhibitory effect on bacteria and cancer cell lines. The half-maximal inhibitory concentration of silver nanoparticles for *Pseudomonas aeruginosa* and MCF7 is 0.30 and 9.44 mg/L, respectively. Additionally, the visible photoluminescence emission of the biosynthesized silver nanospheres has been recorded at the wavelength range of 500-600 nm, indicating that plant extract-mediated silver nanoparticles are useful for fabricating biosensors.

Keywords: antimicrobial activity; blue light-emitting diode; *Durio zibethinus* peel; photoluminescence emission; silver nanoparticles.

1. Introduction

Silver nanomaterials have been an attractive research object for many scientists around the world because of their special characteristics and applications in many fields, such as chemistry [1], medicine [2], microbiology [3], and technology [4]. Among them, silver nanoparticles (AgNPs) are known as metals and have many applications in microbiology. Normally, AgNPs with a size of about 1-100 nm are used in various biomedicine as antifungal [5, 6], antibacterial [7, 8], and inhibitory agents for cancer cells [9-11]. The characteristics and durability of AgNPs depend on many factors, such as shape, size, charges, and particle size distribution [12]. Therefore, numerous methods have been developed to control the properties and stability of AgNPs well, such as chemical, physical, and green chemical synthesis [13]. The general principle for synthesizing AgNPs is to transfer silver ions to silver atoms [14]. For chemical synthesis, chemical-reducing agents such as sodium citrate, sodium borohydride, and hydrazine are often used [15, 16]. However, these reducing agents are toxic and environmental pollution, limiting their application in microbiology [13]. In terms of physical methods,

physical agents for AgNPs conversion, such as electrical discharge [17], heat [4], electromagnetic irradiation [18], and plasma [19], consume a huge of energy, and the cost of equipment is quite expensive. In addition, AgNPs are prone to agglomeration due to a lack of stabilizing agents. Therefore, AgNPs phytosynthesis is gradually becoming a new research trend and receiving attention [20]. Plant extract-based synthesis of AgNPs is considered to have outstanding advantages such as environmental friendliness, simple process, and ease of implementation. In particular, the agents present in the extract play reductants and stabilizers [21].

Durio zibethinus (*D. zibethinus*) is a tropical fruit that is quite popular in Southeast Asian countries such as Thailand, Vietnam, Malaysia, and the Philippines, and it has a distinctive flavor [22]. In Vietnam, *D. zibethinus* production is increasing and is considered a source of income for farmers in fruit-growing regions. The weight of a *D. zibethinus* fruit weighs from 1 to 3 kg, and the peel accounts for about 60-70% of the fruit's weight. The vast amount of waste in the form of peel produced by local markets and processing enterprises can largely be incinerated or disposed of in landfills, creating a large amount of agricultural waste [23]. As part of efforts to reduce food waste, many investigations on using *D. zibethinus* peels to transform them into valuable materials have been published as Alzahrani's research. AgNPs had an average size of about 25 nm and were used to detect the presence of ammonia at low concentrations. The results demonstrate that the synthesized AgNPs could detect ammonia at a concentration of 500 ppm [24]. The research of Chutrakulwong successfully synthesized AgNPs using *D. zibethinus* peel extract under sunlight irradiation; green-synthesized AgNPs were spherical with a size of about 11 nm [25]. The chemical composition of *D. zibethinus* peels contains various phenolics, sugar, and pectin [26]. These are believed to be suitable phytochemicals for forming and stabilizing AgNPs. Pectin and phenolics have been recently researched for the synthesis of metal nanoparticles. The hydroxyl groups of phenolics and pectin are capable of participating in the synthesis and stabilization of AgNPs [27]. Besides the selection of effective reducing and stabilizing agents from plant extracts, the photosynthesis of metal ions was also developed with the assistance of light sources such as fluorescent light [28], light-emitting diodes [29], laser [30], and sunlight [31].

Furthermore, light-emitting diode (LED) light irradiation is beneficial to the formation of AgNPs. However, the use of *D. zibethinus* peel extract combined with blue LED light irradiation for the synthesis of AgNPs and investigation of the storage time of the synthesized AgNPs has not been researched. Therefore, a simple method to synthesize AgNPs using the extract from *D. zibethinus* peels under irradiation of blue LED light was performed in this research. The influence of reaction conditions on the AgNPs synthesis, such as extract concentration, temperature extraction, time extraction, and irradiation time, was researched. The antimicrobial activity of the formed AgNPs was investigated on gram-negative bacteria (*Pseudomonas aeruginosa*, *Escherichia coli*, and *Salmonella enterica*), gram-positive bacteria (*Bacillus subtilis*, *Lactobacillus fermentum*, and *Staphylococcus aureus*), fungi (*Candida albicans*), and cancer cells (A549, Hep-G2, KB, and MCF-7).

2. Materials and Methods

2.1. Materials.

D. zibethinus peels were collected from the local market in Can Tho City. The following step was to cut off the outermost layer and collect the white part, including the intermediate

and innermost layers. After that, the obtained white part of the peels was cut into small pieces, dried, and ground into powder to prepare the extract. AgNPs were green-synthesized using the precursor silver nitrate ($AgNO_3$, 99.9%, Merck). The extraction solvent was double-distilled water.

2.2. Preparing extract and photosynthesizing silver nanospheres.

Different concentrations of *D. zibethinus* peel (C_{Dz}) were extracted in 100 mL of double-distilled water at extraction temperature (T) for extraction duration (t) to obtain extraction mixtures. Once complete, the mixtures were filtered through Whatman filter paper and centrifuged at 3000 rpm for 30 min to remove the solids. The resulting extracts were immediately applied to the following experiments. To keep the Ag^+ concentration at 1 mM, 6.8 mg of silver nitrate was dissolved in 40 mL of *D. zibethinus* peel extract. The light yellow solution became reddish-orange with suitable reaction times, demonstrating AgNPs formation. The presence of phytochemicals in *D. zibethinus* peel extract was used as a reductant and stabilizer for AgNPs synthesis. Moreover, forming AgNPs is promoted and enhanced under blue LED irradiation (20 W and λ = 400-450 nm). Therefore, the effects of various factors on the extract's phytochemicals and the rate of AgNPs formation, including *D. zibethinus* peel concentration, extraction temperature, extraction time, and irradiation time, were carefully examined. Optimization of the nanosilver synthesis through operated parameters such as extract concentration of *D. zibethinus* peel (C_{Dz} = 1, 3, 5, 7, and 9 g/L), extraction temperature (T = 30, 40, 50, 60, and 70°C), extraction time (t = 5, 10, 20, 30, 45, and 60 min) and reaction time occurs with irradiation of blue LED light (t_{ir} = 5, 10, 20, 30, 45, 60, 90, 120, and 150 min). AgNPs formed at optimal parameters were denoted as AgNPsDzL.

2.3. Analyzing.

The use of an ultraviolet-visible (UV-Vis, Jasco Model V730) spectrophotometer in the range of 300-700 nm was used to determine the presence of the produced AgNPs. The photoluminescence emission spectra of AgNPsDzL dispersed in distilled water were recorded by a spectrofluorometer (PL, Horiba Scientific FluoroMax-4) with excitation wavelengths (320-350 nm) at room temperature. The zeta instrument Zetasizer SZ-100 (Horiba, Japan) was utilized to measure the zeta potential of the synthesized AgNPsDzL. A Bruker D2 Phaser X-ray Diffractometer with Cu Kα excitation at 40 mA and 40 kV was used to validate the crystalline phase of the prepared AgNPsDzL. The diffraction intensity is measured at an angle of 2θ between 10 and 80°. Fourier-transform infrared spectroscopy (FTIR, Thermo Nicolet 6700) was used to examine the chemical constituents and functional groups in the *D. zibethinus* peel extract. The size and morphology of the formed AgNPs were determined by Transmission electron microscopy (TEM, JEOL 1400) operating at 120 kV. The presence of Ag^+ was measured on inductively coupled plasma optical emission spectroscopy (ICP-OES, Model 5800, Perkin Elmer) to evaluate the synthesis efficiency of AgNPsDzL.

2.4. Antibacterial and antifungal activity.

Reference strains were utilized in antibacterial testing, and these varieties were gram-positive bacteria: *Lactobacillus fermentum (L. fermentum)* N4, *Bacillus subtilis (B. subtilis)* ATCC 6633, *Staphylococcus aureus (S. aureus)* ATCC 13709 and gram-negative bacteria: *Pseudomonas aeruginosa (P. aeruginosa)* ATCC 15442, *Escherichia coli (E. coli)* ATCC

25922, and *Salmonella enterica (S. enterica)* ATCC 35664 using the dilution technique. For bacteria, tryptic soy agar and broth were utilized for pre-cultivation. Using MacFarland's standards, pathogen cultures were conducted for 24 h at 37°C to achieve 5×10^5 CFU/mL. Gram-positive and gram-negative bacteria are controlled by ampicillin and cefotaxime, respectively. The 50% inhibitory concentration (IC_{50}) of the formed AgNPs was determined using 96-well microplates, and absorbance was measured at 630 nm.

2.5. Anticancer activity.

The plant-mediated AgNPs were applied to test on A549, Hep-G2, KB, and MCF-7 cell lines. To investigate the inhibition activity of the cancer cell growth, various concentrations: 0.97, 3.88, 15.51, and 62.05 mg/L were prepared. The concentrations were diluted by a solvent named dimethyl sulfoxide (DMSO). The cells were subsequently incubated with 5% CO_2 for 72 h. In the next stage, the incubated cells continued to add 100 mg/ml MTT reagent and incubated at 37°C for 4 h. In order to make the produced formazan soluble, 100 µl of DMSO was added. In this study, ellipticine was employed as the control substance. 96-well plates were used to perform absorbance measurements at 540 nm.

Testing for investigating antibacterial and anticancer activity has proceeded thrice for repetitions. Moreover, GraphPad Prism software was used to calculate means and standard deviations.

3. Results and Discussion

3.1. Synthesizing AgNPsDzL.

Several samples including 1 mM $AgNO_3$ solution (Ag), 3 g/L of *D. zibethinus* peel extracted at 60°C for 30 min (Dz), 1 mM $AgNO_3$ dissolved in Dz and stirred for 2 h (Ag-Dz), and solution of 1 mM $AgNO_3$ and Dz irradiated by blue LED light for 2 h (Ag-Dz-L) were prepared to initially investigate the role of *D. zibethinus* peel extract as well as irradiation. Figure 1 illustrates the UV-Vis spectra of the prepared samples. AgNPs synthesis was investigated using peel extract of *D. zibethinus*. Observe the color change of *D. Zibethinus* peel extract when $AgNO_3$ was added; the solution changes from yellowish to orange-brown, indicating the formation of AgNPs. The AgNPs formation was determined by a maximum absorption wavelength of 423 nm on Ag-Dz and Ag-Dz-L. This survey result is completely consistent with previous studies of Dzul-Erosa and Patil; the synthesis of AgNPs was validated through surface plasmon resonance (SPR) with maximum absorbance between 400 and 450 nm [32, 33]. This proves that AgNPs were formed in the reaction solution. The case of $AgNO_3$ solution (Ag) and *D. zibethinus* peel extract (Ext) did not exhibit absorption peaks. Phytochemicals like phenolics, flavonoids, terpenoids, amino acids, and alcohol were used in the bioreduction of AgNPs [34]. From the survey results, the phenolics and flavonoids in the *D. zibethinus* peel extract may have participated in the formation of AgNPs as reducing agents and stabilizers throughout the synthesis process. As can be seen, the absorbance of Ag-Dz-L was higher than that of Ag-Dz (0.367 compared to 0.237), which means that more AgNPs were produced with the assistance of blue LED light than without irradiation. This can be explained by the SPR phenomenon occurring when irradiating blue LED light with a maximum wavelength in the range of 400-450 nm [35]. This shows that the formation of AgNPs was highly dependent on the exposure wavelength of the blue LED light. This demonstrated the role and effect of blue LED exposure in the Ag^+ to Ag^0 conversion process. The parameters

affecting the synthesis of AgNPs were researched in the concentration of *D. zibethinus* peel extract (2.5, 5.0, 7.5, 10.0, and 12.5 g/L), temperature extraction (30, 40, 50, 60, and 70°C), extraction time (10, 20, 30, 40, and 50 min), and blue LED light irradiation time (5, 10, 20, 30, 45, 60, 90, 120, and 150 min).

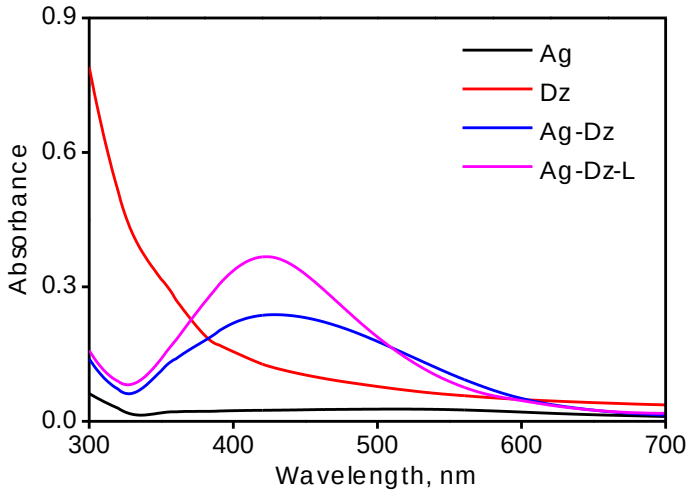

Figure 1. The UV-Vis spectra of the synthesized samples for investigating the function of *D. zibethinus* peel extract and blue LED light.

Several samples including 1 mM $AgNO_3$ solution (Ag), 3 g/L of *D. zibethinus* peel extracted at 60°C for 30 min (Dz), 1 mM $AgNO_3$ dissolved in Dz and stirred for 2 h (Ag-Dz), and solution of 1 mM $AgNO_3$ and Dz irradiated by blue LED light for 2 h (Ag-Dz-L) were prepared to initially investigate the role of *D. zibethinus* peel extract as well as irradiation. Figure 1 illustrates the UV-Vis spectra of the prepared samples. AgNPs synthesis was investigated using peel extract of *D. zibethinus*. Observe the color change of *D. Zibethinus* peel extract when $AgNO_3$ was added; the solution changes from yellowish to orange-brown, indicating the formation of AgNPs. The AgNPs formation was determined by a maximum absorption wavelength of 423 nm on Ag-Dz and Ag-Dz-L. This survey result is completely consistent with previous studies of Dzul-Erosa and Patil; the synthesis of AgNPs was validated through surface plasmon resonance (SPR) with maximum absorbance between 400 and 450 nm [32, 33]. This proves that AgNPs were formed in the reaction solution. The case of $AgNO_3$ solution (Ag) and *D. zibethinus* peel extract (Ext) did not exhibit absorption peaks. Phytochemicals like phenolics, flavonoids, terpenoids, amino acids, and alcohol were used in the bioreduction of AgNPs [34]. From the survey results, the phenolics and flavonoids in the *D. zibethinus* peel extract may have participated in the formation of AgNPs as reducing agents and stabilizers throughout the synthesis process. As can be seen, the absorbance of Ag-Dz-L was higher than that of Ag-Dz (0.367 compared to 0.237), which means that more AgNPs were produced with the assistance of blue LED light than without irradiation. This can be explained by the SPR phenomenon occurring when irradiating blue LED light with a maximum wavelength in the range of 400-450 nm [35]. This shows that the formation of AgNPs was highly dependent on the exposure wavelength of the blue LED light. This demonstrated the role and effect of blue LED exposure in the Ag^+ to Ag^0 conversion process. The parameters affecting the synthesis of AgNPs were researched in the concentration of *D. zibethinus* peel extract (2.5, 5.0, 7.5, 10.0, and 12.5 g/L), temperature extraction (30, 40, 50, 60, and 70°C), extraction time (10, 20, 30, 40, and 50 min), and blue LED light irradiation time (5, 10, 20, 30, 45, 60, 90, 120, and 150 min).

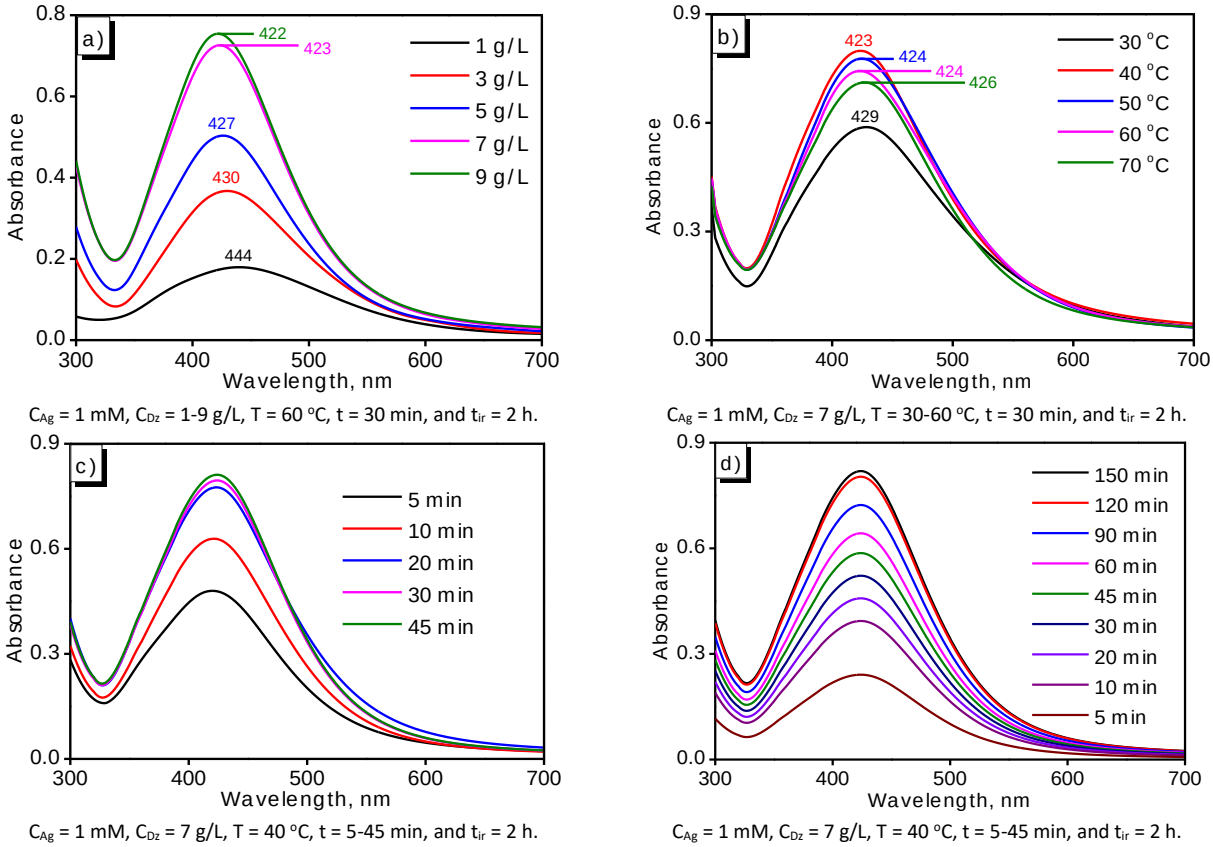

C_{Ag} = 1 mM, C_{Dz} = 1-9 g/L, T = 60 °C, t = 30 min, and t_{ir} = 2 h.

C_{Ag} = 1 mM, C_{Dz} = 7 g/L, T = 30-60 °C, t = 30 min, and t_{ir} = 2 h.

C_{Ag} = 1 mM, C_{Dz} = 7 g/L, T = 40 °C, t = 5-45 min, and t_{ir} = 2 h.

C_{Ag} = 1 mM, C_{Dz} = 7 g/L, T = 40 °C, t = 5-45 min, and t_{ir} = 2 h.

Figure 2. The influence of parameters on the AgNPsDzL production: concentration of **(a)** *D. zibethinus* peel; **(b)** extraction temperature; **(c)** extraction time; **(d)** irradiation time.

The effect of the *D. zibethinus* peel concentration was surveyed at concentrations from 1 to 9 g/L and is shown in Figure 2a. The absorption intensity increased and shifted to lower wavelengths as *D. zibethinus* peel concentration increased from 1 to 9 g/L. A lack of reducing agents and stabilizers at a low concentration (1 g/L) led to a low quantity of larger AgNPs formation with SPR at 444 nm. Meanwhile, more AgNPs were produced by increasing the concentration from 3 to 5 g/L. It is easy to see there was a blueshift of SPR to a lower wavelength (430 and 427 nm), and absorbance increased roughly 2-3 times compared with 1 g/L of *D. zibethinus* peel. Alternatively, reductants and stabilizers were effectively maintained for the AgNPs production at high concentrations (7 and 9 g/L). It is known that absorbance and SPR rise slightly. Based on the results in Figure 2a, it was found that 7 g/L of the *D. zibethinus* peel is optimal for synthesizing AgNPs.

The effect of temperature on the extraction process was studied in turn at different temperatures (30-70°C) for 30 min. Figure 2b shows the results of UV-Vis spectra of the synthesized samples; the concentration of *D. zibethinus* peel and $AgNO_3$ was maintained at 7 g/L and 1 mM, respectively. Compared to other temperatures, 40°C is a suitable temperature for extraction since a proper amount of reductants and stabilizers were generated, resulting in high absorbance in samples extracted at 40°C. According to Desai, AgNPs can be combined with undesirable organic compounds in the extract if the extraction temperature is high [36]. The obtained results in this experiment also show that there was a shift to larger wavelengths and a decrease in absorbance for samples extracted at a range temperature of 50-70°C. Temporarily, the extract was prepared at 30°C, and it contained a few phytochemicals, leading to a shortage of agents for reducing and stabilizing AgNPs. This was presented in the lowest absorbance of AgNPs and highest SPR at 429 nm compared to other samples extracted at 40-70°C. It was found that the appropriate temperature for extracting *D. zibethinus* to synthesize

AgNPs was 40°C.

The effect of extraction time on synthesis was investigated at time intervals of 5-45 min. The absorbance of samples bio-synthesized at various extraction times is shown in Figure 2c. When the reaction time increased, the position of SPR was almost unchanged. However, there was an increase in the intensity with extraction time. This indicates that increasing the extraction time from 5 to 45 min promoted a rise in the amount of phytochemicals produced, which was beneficial for AgNPs formation. This trend was also shown in Vishwasrao's study on *Kalipatti sapodilla* fruit for AgNPs synthesis [37]. Additionally, the extraction time was prolonged, reducing AgNPs formation caused by promoting the desorption of biomolecules [38]. Therefore, the suitable extraction time to synthesize metallic nanoparticles was 20 min.

The role of blue LED light in the synthesis of AgNPs was confirmed in Figure 2d. The previous studies indicated that the morphology of AgNPs can be controlled by photochemical synthesis [39, 40]. When excited by light, metal nanoparticles create an electromagnetic field around the excited particles. When the frequency of the incident light is equal to the vibration frequency of the plasmons, the incident electromagnetic radiation interacts with the plasmon oscillations, resulting in surface plasmon resonance excitation [41]. The blue LED light used in this experiment has a maximum wavelength in the range of 400-450 nm; the maximum absorption of AgNPs coincides with the maximum emission of blue LED light, leading to the effect of the SPR phenomenon [35]. Therefore, the irradiation of blue LED light and the irradiation time will affect the synthesis of AgNPs because of the high coupling of AgNPs to particular wavelengths of incident light. The influence of blue LED light irradiation time on the synthesis of AgNPs was investigated with time intervals varying from 5 to 150 min. Figure 2d indicates the irradiation time of the blue LED light during the formation of AgNPs. When the blue LED's irradiation time increased, the absorption peak's intensity increased with the unchanging of the SPR position. The obtained results show that the optimal LED light irradiation time for the material synthesis was 120 min.

Considering the synthesized results shown in Figure 2, it was obvious that the ideal parameters for synthesizing AgNPs were 7 g/L of *D. zibethinus* peel extracted at 40°C for 20 min, and reaction time occurred with 120-minute irradiation of blue LED light. A sample of AgNPs synthesized at optimal factors was designated as AgNPsDzL.

The efficiency of AgNPsDzL synthesis using *D. zibethinus* peel extract under blue LED irradiation was determined by Ag^+ concentration in the precursor and AgNPsDzL. The results were calculated according to equation (1), and Table 1 indicated that the AgNPsDzL synthesis yield was 88.0%.

$$H = 100 \times \frac{C_o - C}{C_o} (1)$$

where C_o and C are the concentrations of Ag^+ in the precursor and the synthesized AgNPs solution, respectively, and H is the reaction efficiency of AgNPs.

Table 1. The concentration of Ag^+ from ICP measurement.

Sample	Ag^+ concentration, mg/L	Reaction efficiency, %	AgNPs concentration, mg/L
Precursor	86.8		
AgNPsDzL	10.4	88.0	76.4

3.2. Characterization of AgNPsDzL.

AgNPsDzL sample was stored at room temperature for 10 weeks to determine AgNPs

concentration through UV-Vis spectra. The results in Figure 3 show that AgNPs were further formed over storage time. The reason was continuing to convert into AgNPs of residue Ag^+ and the phytochemicals in the AgNPsDzL solution. In addition, the SPR of the studied sample was an insignificant shift during 10 weeks, ranging from 422.8-424.0 nm. From the obtained results, the AgNPsDzL sample was stable at room temperature for a long time.

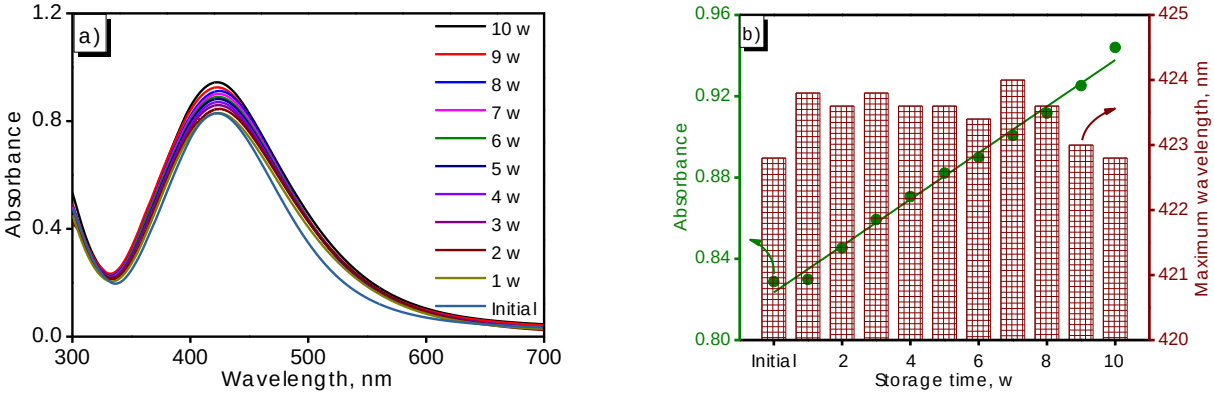

Figure 3. (a) UV-Vis; **(b)** maximum wavelength of AgNPsDzL at numerous storage times.

The XRD pattern in Figure 4a illustrates the structure of AgNPsDzL. The crystal facets (111), (200), (220), and (311) were represented for diffraction peaks at 2θ = 38.13, 44.18, 64.48, and 77.44°, respectively. AgNPsDzL material had the largest (111) plane diffraction. Peaks were indexed using a face-centered cubic (FCC) silver lattice and were perfectly compatible with JCPDS No. 04-0783 standard data. It can be seen from the XRD result that the nanomaterial formed by *D. zibethinnus* peel extract under blue LED irradiation was completely pure silver. Using the Debye-Scherrer equation, the average crystallite size was calculated by formula (2) from the FWHM of the diffraction peaks.

$$D = \frac{K \times \lambda}{\beta \times \cos\theta} (2)$$

where the crystallite size is D, the peak width at half maximum (FWHM) is β radians, the diffraction peak position is θ, and K is the Scherrer constant (K = 0.94). Using Origin 9.0 software, the FWHM was calculated from a Gaussian fit to the four peaks (111), (200), (220), and (311). According to Table 2, the average AgNPsDzL crystallite size was 14.4 nm.

Table 2. The phase composition and crystallite size of AgNPsDzL.

2θ (o)	FWHM	Particle size (nm)	Average particle size (nm)
38.13	0.630	13.3	14.4
44.18	0.821	10.4	
64.48	0.540	17.4	
77.44	0.627	16.2	

The TEM image of the AgNPsDzL sample in Figure 4b shows that nanospheres constituted the synthesized material. The formed nanoparticles were evenly dispersed and individually put together. The predominant morphology of AgNPsDzL was spherical, with an average size of 13.3 nm, with a size distribution ranging from 6 to 22 nm (Figure 4c).

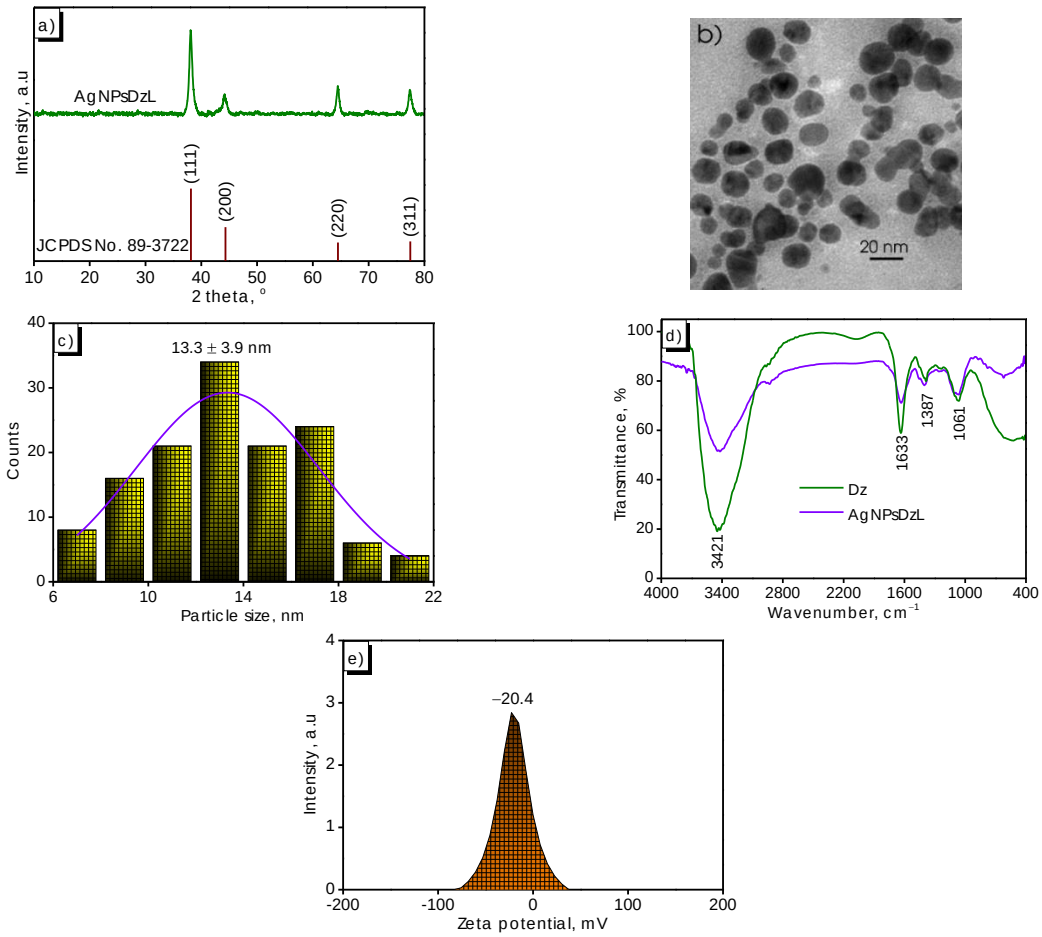

Figure 4. (a) XRD pattern; **(b)** TEM images; **(c)** distribution size; **(d)** FTIR spectra; **(e)** potential zeta of the synthesized AgNPsDzL.

Figure 4d indicates the FTIR spectra of *D. zibethinus* peel extract and the bio-synthesized AgNPs. The FTIR of Dz exhibited absorption peaks at 1061, 1387, 1633, and 3421 cm^{-1} assigned to C-O-C symmetrical stretching modes, stretching vibration of cyclic C-C=C, O-H bending of water, and O-H stretching band [42]. The presence of organic functional groups on the surface of AgNPsDzL was completely similar to the Dz sample. However, there was a lower intensity of the characteristic peaks. A primary reason may be due to the phytochemicals in the *D. zibethinus* peel extract reducing Ag^{+} to Ag^{0}. Also, the obtained results from FTIR spectra show that the phytoconstituents stabilized AgNPs by a coating on the surface of AgNPs to prevent agglomeration [27].

The factor that determines the surface charge of a material is the presence of a stabilizer [43]. Furthermore, the zeta potential of the material demonstrated a measurable indicator of nanoparticle stability. According to Filip's research, metallic nanoparticles possess high long-term stability with zeta potentials in a range of –30 to +30 mV [44]. The colloidal AgNPsDzL prepared in this study exhibited a zeta potential of –20.4 mV, indicating that negative-charged silver nanospheres were long-term stable in the bio-synthesized solution. The negative value of the zeta potential reflects the presence of phytochemicals that help prevent nanoparticle aggregation [45]. The presence of phenolics in *D. zibethinus* peel extract acted as a stabilizer and caused the negative zeta potential of AgNPsDzL [46].

3.3. Applications of AgNPsDzL.

The half-maximum inhibitory concentration (IC_{50}) was used in the study to assess the

inhibitory activity of AgNPsDzL against human pathogenic bacteria. The inhibitory effect and IC_{50} value of AgNPsDzL are shown in Table 3 and Figure 6a. The above results show that formed AgNPsDzL had a good inhibitory ability to inhibit gram-negative bacteria *P. aeruginosa* with IC_{50} = 0.30 mg/L and less effective inhibition against *B. subtilis*. The susceptibility of pathogenic bacteria to AgNPsDzL was shown as follows: *P. aeruginosa* (IC_{50} = 0.30 mg/L) > S. aureus (IC_{50} = 2.27 mg/L) > *L. fermentum* (IC_{50} = 4.23 mg/L) > *S. enterica* (IC_{50} = 5.92 mg/L) > *E. coli* (IC_{50} = 25.38 mg/L). In terms of cancer cell inhibitory activity of AgNPDzL, it was shown in Table 3 and Figure 6b. To analyze the influence of the prepared material on anti-proliferative, the produced AgNPsDzL was used for testing with cancer cell lines such as A549, Hep-G2, KB, and MCF-7 at various concentrations. AgNPsDzL exhibited significant antitumor activity against breast cancer cell line MCF-7 with IC_{50} = 9.44 pM. The sensitivity of cancer cells to AgNPsDzL increased in the order of A549 < Hep-G2 < KB < MCF7. These results suggest that the obtained AgNPsDzL acted as an effective antibacterial/anticancer cell agent.

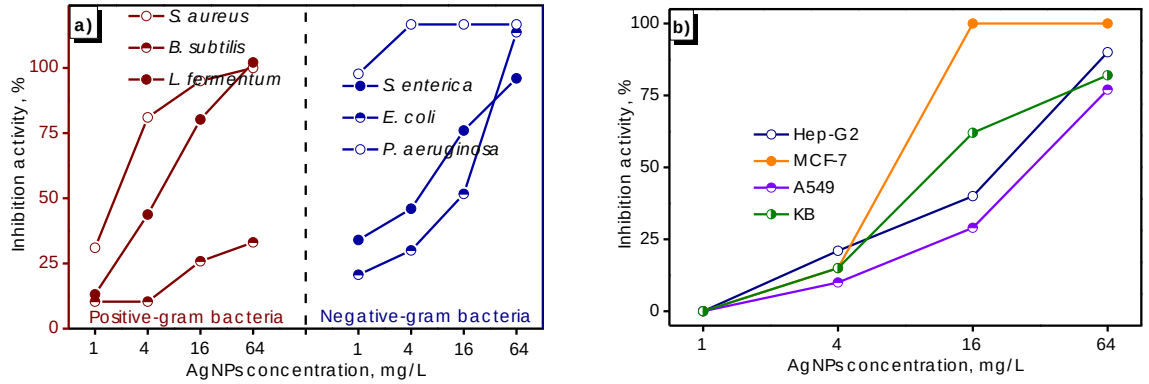

Figure 6. (a) Antibacterial; **(b)** anticancer activity of AgNPsDzL.

Table 3. IC_{50} of AgNPsDzL inhibited the growth of bacteria/fungi/cancer cells.

Bacteria/fungi/cancer cells		**AgNPsDzL (mg/L)**	**Control**		
			Ampicillin (mg/L)	**Cefotaxime (mg/L)**	**Ellipticine (mg/L)**
Negative-gram bacteria	*E. coli*	25.38 ± 1.52		0.12 ± 0.01	
	P. aeruginosa	0.30 ± 0.01		14.32 ± 0.50	
	S. enterica	5.92 ± 0.30		1.42 ± 0.17	
Positive-gram bacteria	*B. subtilis*	–	11.95 ± 1.79		
	L. fermentum	4.23 ± 0.03	3.40 ± 0.23		
	S. aureus	2.27 ± 0.04	0.07 ± 0.02		
Cancer cells	A549	39.12 ± 2.57			1.06 ± 0.07
	Hep-G2	27.07 ± 1.93			1.39 ± 0.13
	KB	13.67 ± 1.25			1.09 ± 0.07
	MCF7	9.44 ± 0.58			1.32 ± 0.10

The fluorescence properties of AgNPsDzL under numerous excitation wavelengths were investigated. The photoluminescence spectra obtained from the synthesized AgNPsDzL are shown in Figure 7. The photoluminescence emission has been found in the visible range of 500 to 600 nm. Peak positions corresponding to 320, 330, 340, and 350 nm excitation wavelengths were found at 545, 545, 557, and 567, respectively. There was a redshifted photoluminescence emission of AgNPsDzL around 10 nm with a crease in excitation wavelength from 330 to 350 nm. Electrons are stimulated to a lower energy level when the excitation wavelength intensifies, emitting these electrons at longer wavelengths. The best fluorescence emission was found with an excitation wavelength of 320 nm.

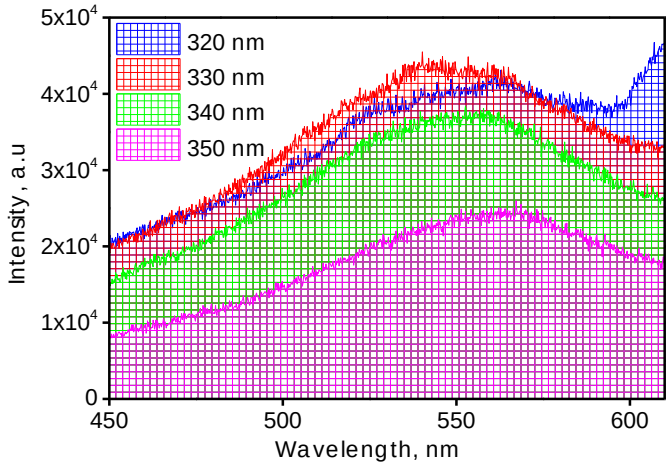

Figure 7. Fluorescence emission spectra of AgNPsDzL at various excitation wavelengths.

Table 4. Compare the results in the present study with other recent studies using *D. zibethinus* peel extract or combined with LED irradiation in AgNPs synthesis.

Plant	Reaction conditions	SPR of AgNPs	Shape, size	Application	Reference
Durio zibethinus	0.1 g/mL *Durio zibethinus* leaf extract, 1 mM $AgNO_3$, irradiated by direct sunlight	415 nm	Spherical, 10-50 nm	- Degradation of organic dyes: methylene blue, coomassie blue, crystal violet, malachite green, methyl red, congo red, rhodamine B, methyl orange, eosin yellow - Reduction of nitroaromatic compounds: 4-nitrophenol, 2-nitroaniline, 4-nitroaniline - Antibacterial activity: *Escherichia coli*, *Staphylococcus aureus* - Colorimetric sensor: Hg^{2+}	[47]
Durio zibethinus	*Durio zibethinus* peel extract, 1 mM $AgNO_3$, pH = 8.5, irradiation of compact fluorescent light bulb	428 nm	Spherical, 5-17 nm	-	[25]
Durio zibethinus	*Durio zibethinus* seed extract, 1.5 mM $AgNO_3$, irradiated by sunlight	420 nm	Spherical and rod-shaped, 20-75 nm	Antibacterial activity: *Staphylococcus aureus, Escherichia coli, Bacillus subtilis*	[48]
Piper longum	*Piper longum* catkin extract, 1 mM $AgNO_3$, irradiated by direct sunlight	450 nm	Spherical, 15-40 nm	Antibacterial activity: *Staphylococcus aureus, Pseudomonas aeruginosa, Bacillus subtilis*	[49]
Durio zibethinus	7 g/L *D. zibethinus* peel extracted, 1 mM $AgNO_3$ irradiation of blue LED light	423 nm	Spherical, 6-22 nm	- Antibacterial activity: *Pseudomonas aeruginosa, Staphylococcus aureus, Lactobacillus fermentum, Salmonella enterica*, *Escherichia coli*; MCF-7, KB, Hep-G2, A549. - Fluorescence properties at excitation wavelength from 330 to 350 nm	This work

A comparison of the results of some other studies using extracts from *D. zibethinus* or combined with blue LED light irradiation to synthesize AgNPs with this study is presented in Table 4. It shows that many studies have used light irradiation to synthesize AgNPs. However, there have not been many studies on the use of blue LED light irradiation. In our study, the synthesized silver nanoparticles have a spherical shape with sizes from 6 to 22 nm, SPR at a wavelength of 423 nm, similar to the results of research on synthesizing AgNPs using *Durio zibethinus* peel and seed extract, *Piper longum* catkin extract combined with irradiation of various lights. Blue LED light irradiation shortened the reaction time and produced more AgNPs. Furthermore, no investigations have evaluated the synthesis efficiency, durability over

storage time, and cell inhibition ability of AgNPs synthesized from *Durio zibethinus* peel extract combined with blue LED light irradiation.

4. Conclusions

Plant extract-assisted photosynthesis of silver nanospheres using *D. zibethinus* peel extract and blue LED light irradiation has been produced with numerous benefits, including eco-friendly, cost-saving, and easy-to-obtain materials. UV-Vis, XRD, and TEM analysis confirmed the formation of the synthesized AgNPsDzL. The irradiation of blue LED light shortened the synthesis process, and the agricultural waste *D. zibethinus* peel was utilized to generate a useful nanomaterial. The plant-assisted AgNPsDzL exhibited as an effective agent for inhibitory bacterial/cancer cell growth. Furthermore, AgNPsDzL were extremely useful in manufacturing biosensor devices based on fluorescence properties.

Funding

This research was funded in part by the Can Tho University, Code: TSV2023-24.

Acknowledgments

This work was supported by the Can Tho University.

Conflicts of Interest

The authors declare no conflict of interest.

References

1. Zahoor, M.; Nazir, N.; Iftikhar, M.; Naz, S.; Zekker, I.; Burlakovs, J.; Uddin, F.; Kamran, A.W.; Kallistova, A.; Pimenov, N.; Ali Khan, F. A Review on Silver Nanoparticles: Classification, Various Methods of Synthesis, and Their Potential Roles in Biomedical Applications and Water Treatment. *Water* **2021**, *13*, 2216, https://doi.org/10.3390/w13162216.
2. Caldonazo, A.; Almeida, S.L.; Bonetti, A.F.; Lazo, R.E.L.; Mengarda, M.; Murakami, F.S. Pharmaceutical applications of starch nanoparticles: A scoping review. *Int. J. Biol. Macromol.* **2021**, *181*, 697-704, https://doi.org/10.1016/j.ijbiomac.2021.03.061.
3. Saravanan, A.; Kumar, P.S.; Karishma, S.; Vo, D.-V.N.; Jeevanantham, S.; Yaashikaa, P.R.; George, C.S. A review on biosynthesis of metal nanoparticles and its environmental applications. *Chemosphere* **2021**, *264*, 128580, https://doi.org/10.1016/j.chemosphere.2020.128580.
4. Pryshchepa, O.; Pomastowski, P.; Buszewski, B. Silver nanoparticles: Synthesis, investigation techniques, and properties. *Adv. Colloid Interface Sci.* **2020**, *284*, 102246, https://doi.org/10.1016/j.cis.2020.102246.
5. Zhang, X.-F.; Liu, Z.-G.; Shen, W.; Gurunathan, S. Silver Nanoparticles: Synthesis, Characterization, Properties, Applications, and Therapeutic Approaches. *Int. J. Mol. Sci.* **2016**, *17*, 1534, https://doi.org/10.3390/ijms17091534.
6. Mussin, J.; Giusiano, G. Biogenic silver nanoparticles as antifungal agents. *Front. Chem.* **2022**, *10*, 1023542, https://doi.org/10.3389/fchem.2022.1023542.
7. Behra, R.; Sigg, L.; Clift, M.J.D.; Herzog, F.; Minghetti, M.; Johnston, B.; Petri-Fink, A.; Rothen-Rutishauser, B. Bioavailability of silver nanoparticles and ions: from a chemical and biochemical perspective. *J. R. Soc. Interface* **2013**, *10*, 20130396, https://doi.org/10.1098/rsif.2013.0396.
8. Li, P.; Li, J.; Wu, C.; Wu, Q.; Li, J. Synergistic antibacterial effects of β-lactam antibiotic combined with silver nanoparticles. *Nanotechnology* **2005**, *16*, 1912, https://doi.org/10.1088/0957-4484/16/9/082.
9. Venugopal, K.; Rather, H.A.; Rajagopal, K.; Shanthi, M.P.; Sheriff, K.; Illiyas, M.; Rather, R.A.; Manikandan, E.; Uvarajan, S.; Bhaskar, M.; Maaza, M. Synthesis of silver nanoparticles (AgNPs) for anticancer activities (MCF7 breast and A549 lung cell lines) of the crude extract of *Syzygium aromaticum*. *J.*

Photochem. Photobiol. B: Biol. **2017**, *167*, 282-289, https://doi.org/10.1016/j.jphotobiol.2016.12.013.
10. Bao, J.; Jiang, Z.; Ding, W.; Cao, Y.; Yang, L.; Liu, J. Silver nanoparticles induce mitochondria-dependent apoptosis and late non-canonical autophagy in HT-29 colon cancer cells. *Nanotechnol. Rev.* **2022**, *11*, 1911-1926, https://doi.org/doi:10.1515/ntrev-2022-0114.
11. Wypij, M.; Jędrzejewski, T.; Trzcińska-Wencel, J.; Ostrowski, M.; Rai, M.; Golińska, P. Green Synthesized Silver Nanoparticles: Antibacterial and Anticancer Activities, Biocompatibility, and Analyses of Surface-Attached Proteins. *Front. Microbiol.* **2021**, *12*, 632505, https://doi.org/10.3389/fmicb.2021.632505.
12. Bhattarai, B.; Zaker, Y.; Atnagulov, A.; Yoon, B.; Landman, U.; Bigioni, T.P. Chemistry and Structure of Silver Molecular Nanoparticles. *Acc. Chem. Res.* **2018**, *51*, 3104-3113, https://doi.org/10.1021/acs.accounts.8b00445.
13. Iravani, S.; Korbekandi, H.; Mirmohammadi, S.V.; Zolfaghari, B. Synthesis of silver nanoparticles: chemical, physical and biological methods. *Res. Pharm. Sci.* **2014**, *9*, 385-406.
14. Jiang, X.C.; Chen, C.Y.; Chen, W.M.; Yu, A.B. Role of Citric Acid in the Formation of Silver Nanoplates through a Synergistic Reduction Approach. *Langmuir* **2010**, *26*, 4400-4408, https://doi.org/10.1021/la903470f.
15. Jabeen, S.; Qureshi, R.; Munazir, M.; Maqsood, M.; Munir, M.; Shah, S.S.H.; Rahim, B.Z. Application of green synthesized silver nanoparticles in cancer treatment-a critical review. *Mater. Res. Express* **2021**, *8*, 092001, https://doi.org/10.1088/2053-1591/ac1de3.
16. Dawadi, S.; Katuwal, S.; Gupta, A.; Lamichhane, U.; Thapa, R.; Jaisi, S.; Lamichhane, G.; Bhattarai, D.P.; Parajuli, N. Current Research on Silver Nanoparticles: Synthesis, Characterization, and Applications. *J. Nanomater.* **2021**, *2021*, 6687290, https://doi.org/10.1155/2021/6687290.
17. Ishida, K.; Cipriano, T.F.; Rocha, G.M.; Weissmüller, G.; Gomes, F.; Miranda, K.; Rozental, S. Silver nanoparticle production by the fungus *Fusarium oxysporum*: nanoparticle characterisation and analysis of antifungal activity against pathogenic yeasts. *Mem. Inst. Oswaldo Cruz* **2013**, *109*, 220-228, https://doi.org/10.1590/0074-0276130269.
18. Kang, W.-J.; Cheng, C.-Q.; Li, Z.; Feng, Y.; Shen, G.-R.; Du, X.-W. Ultrafine Ag Nanoparticles as Active Catalyst for Electrocatalytic Hydrogen Production. *ChemCatChem* **2019**, *11*, 5976-5981, https://doi.org/10.1002/cctc.201901364.
19. Kylián, O.; Kuzminova, A.; Štefaníková, R.; Hanuš, J.; Solař, P.; Kúš, P.; Cieslar, M.; Choukourov, A.; Biederman, H. Silver/plasma polymer strawberry-like nanoparticles produced by gas-phase synthesis. *Mater. Lett.* **2019**, *253*, 238-241, https://doi.org/10.1016/j.matlet.2019.06.069.
20. Rafique, M.; Sadaf, I.; Rafique, M.S.; Tahir, M.B. A review on green synthesis of silver nanoparticles and their applications. *Artif. Cells Nanomed. Biotechnol.* **2017**, *45*, 1272-1291, https://doi.org/10.1080/21691401.2016.1241792.
21. Jamkhande, P.G.; Ghule, N.W.; Bamer, A.H.; Kalaskar, M.G. Metal nanoparticles synthesis: An overview on methods of preparation, advantages and disadvantages, and applications. *J. Drug Deliv. Sci. Technol.* **2019**, *53*, 101174, https://doi.org/10.1016/j.jddst.2019.101174.
22. Leontowicz, H.; Leontowicz, M.; Haruenkit, R.; Poovarodom, S.; Jastrzebski, Z.; Drzewiecki, J.; Ayala, A.L.M.; Jesion, I.; Trakhtenberg, S.; Gorinstein, S. Durian (*Durio zibethinus Murr.*) cultivars as nutritional supplementation to rat's diets. *Food Chem. Toxicol.* **2008**, *46*, 581-589, https://doi.org/10.1016/j.fct.2007.08.042.
23. Takolpuckdee, P. Transformation of Agricultural Market Waste Disposal to Biochar Soil Amendments. *Procedia Environ. Sci.* **2014**, *20*, 64-70, https://doi.org/10.1016/j.proenv.2014.03.010.
24. Alzahrani, E. Colorimetric Detection of Ammonia Using Synthesized Silver Nanoparticles from Durian Fruit Shell. *J. Chem.* **2020**, *2020*, 4712130, https://doi.org/10.1155/2020/4712130.
25. Chutrakulwong, F.; Thamaphat, K.; Limsuwan, P. Photo-irradiation induced green synthesis of highly stable silver nanoparticles using durian rind biomass: effects of light intensity, exposure time and pH on silver nanoparticles formation. *J. Phys. Commun.* **2020**, *4*, 095015, https://doi.org/10.1088/2399-6528/abb4b5.
26. Zhan, Y.-f.; Hou, X.-t.; Fan, L.-l.; Du, Z.-c.; Ch'ng, S.E.; Ng, S.M.; Thepkaysone, K.; Hao, E.-w.; Deng, J.-g. Chemical constituents and pharmacological effects of durian shells in ASEAN countries: A review. *Chin. Herb. Med.* **2021**, *13*, 461-471, https://doi.org/10.1016/j.chmed.2021.10.001.
27. Abbai, R.; Mathiyalagan, R.; Markus, J.; Kim, Y.; Wang, C.; Singh, P.; Ahn, S.; Farh, M.E.; Yang, D.C. Green synthesis of multifunctional silver and gold nanoparticles from the oriental herbal adaptogen: Siberian ginseng. *Int. J. Nanomed.* **2016**, *11*, 3131-3143, https://doi.org/10.2147/IJN.S108549.
28. Khamhaengpol, A.; Siri, S. Fluorescent light mediated a green synthesis of silver nanoparticles using the

protein extract of weaver ant larvae. *J. Photochem. Photobiol. B: Biol.* **2016**, *163*, 337-344, https://doi.org/10.1016/j.jphotobiol.2016.09.003.
29. Anjum, S.; Chaudhary, R.; Khan, A.K.; Hashim, M.; Anjum, I.; Hano, C.; Abbasi, B.H. Light-emitting diode (LED)-directed green synthesis of silver nanoparticles and evaluation of their multifaceted clinical and biological activities. *RSC Adv.* **2022**, *12*, 22266-22284, https://doi.org/10.1039/D2RA03503K.
30. Mwenze, N.M.; Juma, M.; Maaza, M.; Birech, Z.; Dhlamini, M.S. Laser liquid ablation for silver nanoparticles synthesis and conjugation with hydroxychloroquine for Covid-19 treatment. *Mater. Today: Proc.* **2023**, https://doi.org/10.1016/j.matpr.2023.08.195.
31. Rizwana, H.; Alwhibi, M.S.; Al-Judaie, R.A.; Aldehaish, H.A.; Alsaggabi, N.S. Sunlight-Mediated Green Synthesis of Silver Nanoparticles Using the Berries of *Ribes rubrum* (Red Currants): Characterisation and Evaluation of Their Antifungal and Antibacterial Activities. *Molecules* **2022**, *27*, 2186, https://doi.org/10.3390/molecules27072186.
32. Dzul-Erosa, M.S.; Cauich-Díaz, M.M.; Razo-Lazcano, T.A.; Avila-Rodriguez, M.; Reyes-Aguilera, J.A.; González-Muñoz, M.P. Aqueous leaf extracts of *Cnidoscolus chayamansa* (Mayan chaya) cultivated in Yucatan Mexico. Part II: Uses for the phytomediated synthesis of silver nanoparticles. *Mater. Sci. Eng. C* **2018**, *91*, 838-852, https://doi.org/10.1016/j.msec.2018.06.007.
33. Patil, M.P.; Kim, G.-D. Eco-friendly approach for nanoparticles synthesis and mechanism behind antibacterial activity of silver and anticancer activity of gold nanoparticles. *Appl. Microbiol. Biotechnol.* **2017**, *101*, 79-92, https://doi.org/10.1007/s00253-016-8012-8.
34. Shaikh, W.A.; Chakraborty, S.; Owens, G.; Islam, R.U. A review of the phytochemical mediated synthesis of AgNP (silver nanoparticle): the wonder particle of the past decade. *Appl. Nanosci.* **2021**, *11*, 2625-2660, https://doi.org/10.1007/s13204-021-02135-5.
35. da Silva, R.T.P.; Petri, M.V.; Valencia, E.Y.; Camargo, P.H.C.; de Torresi, S.I.C.; Spira, B. Visible light plasmon excitation of silver nanoparticles against antibiotic-resistant *Pseudomonas aeruginosa*. *Photodiagnosis Photodyn. Ther.* **2020**, *31*, 101908, https://doi.org/10.1016/j.pdpdt.2020.101908.
36. Desai, R.; Mankad, V.; Gupta, S.K.; Jha, P.K. Size Distribution of Silver Nanoparticles: UV-Visible Spectroscopic Assessment. *Nanosci. Nanotechnol. Lett.* **2012**, *4*, 30-34, https://doi.org/10.1166/nnl.2012.1278.
37. Vishwasrao, C.; Momin, B.; Ananthanarayan, L. Green Synthesis of Silver Nanoparticles Using Sapota Fruit Waste and Evaluation of Their Antimicrobial Activity. *Waste Biomass Valorization* **2019**, *10*, 2353-2363, https://doi.org/10.1007/s12649-018-0230-0.
38. Elemike, E.E.; Onwudiwe, D.C.; Arijeh, O.; Nwankwo, H.U. Plant-mediated biosynthesis of silver nanoparticles by leaf extracts of *Lasienthra africanum* and a study of the influence of kinetic parameters. *Bull. Mater. Sci.* **2017**, *40*, 129-137, https://doi.org/10.1007/s12034-017-1362-8.
39. Lee, S.H.; Jun, B.-H. Silver Nanoparticles: Synthesis and Application for Nanomedicine. *Int. J. Mol. Sci.* **2019**, *20*, 865, https://doi.org/10.3390/ijms20040865.
40. Sritong, N.; Chumsook, S.; Siri, S. Light emitting diode irradiation induced shape conversion of DNA-capped silver nanoparticles and their antioxidant and antibacterial activities. *Artif. Cells Nanomed. Biotechnol.* **2018**, *46*, 955-963, https://doi.org/10.1080/21691401.2018.1439841.
41. Paul, K.K.; Giri, P.K. Plasmonic Metal and Semiconductor Nanoparticle Decorated TiO2-Based Photocatalysts for Solar Light Driven Photocatalysis. In Encyclopedia of Interfacial Chemistry; Wandelt, K., Ed.; Elsevier, Oxford,**2018**; 786-794, https://doi.org/10.1016/B978-0-12-409547-2.13176-2.
42. Elhawary, S.; EL-Hefnawy, N.; Alzahraa, F.A.; Sobeh, M.; Mostafa, E.; Osman, S.; El-Raey, M. Green Synthesis of Silver Nanoparticles Using Extract of *Jasminum officinal* L. Leaves and Evaluation of Cytotoxic Activity Towards Bladder (5637) and Breast Cancer (MCF-7) Cell Lines [Retraction]. *Int. J. Nanomed.* **2022**, *17*, 2805-2806, https://doi.org/10.2147/IJN.S380183.
43. Jayeoye, T.J.; Eze, F.N.; Olatunji, O.J.; Tyopine, A.A. Synthesis of biocompatible Konjac glucomannan stabilized silver nanoparticles, with *Asystasia gangetica* phenolic extract for colorimetric detection of mercury (II) ion. *Sci. Rep.* **2022**, *12*, 9176, https://doi.org/10.1038/s41598-022-13384-x.
44. Filip, G.A.; Moldovan, B.; Baldea, I.; Olteanu, D.; Suharoschi, R.; Decea, N.; Cismaru, C.M.; Gal, E.; Cenariu, M.; Clichici, S.; David, L. UV-light mediated green synthesis of silver and gold nanoparticles using Cornelian cherry fruit extract and their comparative effects in experimental inflammation. *J. Photochem. Photobiol. B: Biol.* **2019**, *191*, 26-37, https://doi.org/10.1016/j.jphotobiol.2018.12.006.
45. Sumitha, S.; Vasanthi, S.; Shalini, S.; Chinni, S.V.; Gopinath, S.C.B.; Kathiresan, S.; Anbu, P.; Ravichandran, V. Durio zibethinus rind extract mediated green synthesis of silver nanoparticles: Characterization and

biomedical applications. *Pharmacogn. Mag.* **2019**, *15*, 52-58, https://doi.org/10.4103/pm.pm_400_18.
46. Wei, X.; Luo, M.; Li, W.; Yang, L.; Liang, X.; Xu, L.; Kong, P.; Liu, H. Synthesis of silver nanoparticles by solar irradiation of cell-free *Bacillus amyloliquefaciens* extracts and $AgNO_3$. *Bioresour. Technol.* **2012**, *103*, 273-278, https://doi.org/10.1016/j.biortech.2011.09.118.
47. Sengan, M.; Veeramuthu, D.; Veerappan, A. Photosynthesis of silver nanoparticles using *Durio zibethinus* aqueous extract and its application in catalytic reduction of nitroaromatics, degradation of hazardous dyes and selective colorimetric sensing of mercury ions. *Mater. Res. Bull.* **2018**, *100*, 386-393, https://doi.org/10.1016/j.materresbull.2017.12.038.
48. Sumitha, S.; Vasanthi, S.; Shalini, S.; Chinni, S.V.; Gopinath, S.C.B.; Anbu, P.; Bahari, M.B.; Harish, R.; Kathiresan, S.; Ravichandran, V. Phyto-Mediated Photo Catalysed Green Synthesis of Silver Nanoparticles Using Durio Zibethinus Seed Extract: Antimicrobial and Cytotoxic Activity and Photocatalytic Applications. *Molecules* **2018**, *23*, 3311, https://doi.org/10.3390/molecules23123311.
49. Jayapriya, M.; Dhanasekaran, D.; Arulmozhi, M.; Nandhakumar, E.; Senthilkumar, N.; Sureshkumar, K. Green synthesis of silver nanoparticles using *Piper longum* catkin extract irradiated by sunlight: antibacterial and catalytic activity. *Res. Chem. Intermed.* **2019**, *45*, 3617-3631, https://doi.org/10.1007/s11164-019-03812-5.